

Photoneutron Cross Sections of Pb^{206} , Pb^{207} , Pb^{208} , and Bi^{209} †

R. R. HARVEY, J. T. CALDWELL, R. L. BRAMBLETT, AND S. C. FULTZ
Lawrence Radiation Laboratory, University of California, Livermore, California
 (Received 13 April 1964)

Cross sections for (γ, n) and $(\gamma, 2n)$ reactions on Pb^{206} , Pb^{207} , Pb^{208} , and Bi^{209} have been measured using monochromatic gamma rays having an energy resolution of 3%. The peak cross sections for $\sigma[(\gamma, n) + (\gamma, np)]$ are 515, 475, 495, and 515 mb, respectively, and for $\sigma(\gamma, 2n)$ are 76, 80, 117, and 105 mb, respectively. Integrated cross sections for $\sigma(\gamma, n)$ up to 28 MeV are 2.22, 2.05, 1.96, and 2.17 MeV-b, while for $\sigma(\gamma, 2n)$ are 0.56, 0.60, 0.95, and 0.76 MeV-b, respectively. Level-density parameters for the residual nuclei Pb^{206} , Pb^{207} , Pb^{208} , and Bi^{209} were found to be 6.6, 13.5, 9.6, and 10.2 MeV⁻¹, respectively, each determined to $\pm 11\%$. Values obtained for σ_{-2} are 15.6, 14.5, 14.1, and 16.6 mb/MeV, respectively.

INTRODUCTION

THE single nucleon differences between Pb^{206} , Pb^{207} , Pb^{208} , and Bi^{209} in the vicinity of the doubly closed shell of Pb^{208} ($N=126$, $Z=82$) offer a series of isotopes of considerable interest in the study of the behavior of the photon absorption cross section in the region of closed shells. These nuclei have been previously studied by a number of investigators, but without the use of separated isotopes with the high enrichment presently available. Photoneutron thresholds for Pb^{206} , Pb^{207} , and Pb^{208} were measured by Palevsky and Hansen¹ who obtained 8.25 ± 0.10 , 6.95 ± 0.10 , and 7.44 ± 0.10 MeV, respectively. Price² measured the angular distribution of photoneutrons from natural Pb using 22-MeV bremsstrahlung. The neutron detector used the $\text{Al}(n, p)$ reaction, which is sensitive to neutrons above 1.8 MeV. The angular distribution obtained peaked at 90° and was symmetrical about it. Neutron spectra were also measured by use of thick emulsions and were found to fit the level density distribution

$$W_n(\epsilon) = C \exp 2(a\epsilon)^{1/2}, \quad (1)$$

where ϵ denotes energy and a is the level density parameter. Toms and Stephens³ measured the photoproton spectrum and angular distribution for Pb^{208} by use of bremsstrahlung and thick emulsions. They found that the proton yield was approximately 1300 times greater than that predicted from evaporation theory, which indicated considerable direct interaction. Also, the angular distribution of the protons was not symmetrical about 90° , but was peaked forward at approximately 50° . This seemed to indicate considerable shell structure effect. Later the same authors⁴ measured the angular distribution of the photoneutrons emitted by lead. They found a small anisotropic component in the neutron angular distribution. The best fit to the neutron spectrum was obtained with the level density of Eq. (1) using the level density parameter, $a=14$

MeV⁻¹. They obtained a 10% contribution from direct photoneutrons. They also measured the cross section for photoneutron production and obtained the following characteristics for the giant resonance: Peak cross section of 550 mb at 13.8 MeV with a width at half-maximum Γ of 2.4 MeV.

Fuller and Hayward⁵ measured elastic scattering and photoneutron cross sections for Pb^{206} , Pb^{207} , Pb^{208} , and Bi^{209} . They observed identical cross sections between 10 and 14 MeV, but differences below and above this region. The peak cross section for all measurements was 900 mb, occurring at 13.5 MeV with a width at half-maximum of 3.8 MeV. The integrated cross section was 3.93 MeV-b. In addition, all cross-section curves gave indications of a shoulder at 12 MeV and a dip at approximately 8.2 MeV. Miller, Schuhl, and Tzara⁶ measured the photoneutron cross section for natural lead for photon energies up to 22 MeV, using nearly monochromatic photons obtained from the annihilation-in-flight of fast positrons. They obtained a peak cross section of approximately 600 mb at 13.8 MeV with a Γ of 4.8 MeV and an integrated cross section of 4.10 MeV-b.

Additional measurements on the photoproton cross section of Pb^{207} were made by Sorokin, Shevchenko, and Yur'ev⁷ who measured the activation Tl^{206} obtained from the $\text{Pb}^{207}(\gamma, p)\text{Tl}^{206}$ reaction. The (γ, p) integrated cross section up to 32 MeV was found to be approximately 55 MeV-mb. The fraction of quadrupole absorption was estimated at about 50%.

EXPERIMENTAL METHOD

For the present work the source of radiation used was essentially monochromatic photons of variable energy obtained from the annihilation-in-flight of fast positrons. The positrons were created by pair production from 10-MeV bremsstrahlung in a thick tungsten target located at the end of the first section of a three-section linear electron accelerator. They were ac-

† Work done under the auspices of the U. S. Atomic Energy Commission.

¹ H. Palevsky and A. O. Hansen, *Phys. Rev.* **79**, 242A (1950).

² G. A. Price, *Phys. Rev.* **93**, 1279 (1954).

³ M. E. Toms and W. E. Stephens, *Phys. Rev.* **98**, 628 (1955).

⁴ M. E. Toms and W. E. Stephens, *Phys. Rev.* **108**, 77 (1957).

⁵ E. G. Fuller and E. Hayward, *Nucl. Phys.* **33**, 431 (1962).

⁶ J. Miller, C. Schuhl, and C. Tzara, *Nucl. Phys.* **32**, 236 (1962).

⁷ Yu. I. Sorokin, V. G. Shevchenko, and B. A. Yur'ev, *Zh. Eksperim. i Teor. Fiz.* **43**, 1600 (1962) [English transl.: *Soviet Phys.—JETP* **16**, 1127 (1963)].

celerated to the desired energy by the second and third sections, and were then magnetically analyzed and made to pass through a thin target of LiH. The photons created from the two-photon annihilation of the positrons with the electrons in the target material were selected in the forward direction. The energy resolution of these photons was approximately 3%, although the momentum resolution of the positrons was only 1%.

The photons were measured by use of a thin-walled transmission ion chamber filled with xenon to a pressure of about $\frac{1}{2}$ atm. The ion chamber was calibrated by use of a NaI(Tl) gamma-ray spectrometer and a remotely operated Faraday cup. The sample was located at the center of a 4π paraffin-moderated neutron detector containing 24 BF_3 proportional counters, each filled to a pressure of 120 cm. The photoneutron samples which consisted of metallic disks, each 2 in. in diameter, 0.25 in. thick, were located at the center of the paraffin block in a 3-in.-diam axial hole. Measurements were made simultaneously on the number of gamma rays and the neutron yield for chosen positron energies ranging from 8.5 to 30 MeV. Contributions to the neutron count rate from positron bremsstrahlung were deduced by measuring the neutron yields at similar selected energies when negative electrons were incident upon the LiH target. The effects of positron bremsstrahlung were calculated on the premise that the bremsstrahlung yield per particle from positrons is similar to that obtained from negative electrons.⁸

The neutron detector, which consisted of an 18-in. cube of paraffin, had a decay time of 125 μ sec and an efficiency of 0.20. The gating interval for the scaling circuits was 335 μ sec. Each gating interval was started 8 μ sec after the annihilation-photon burst in order to avoid counting gamma-ray pulses from the neutron detector. The neutron counts were separated electronically as single, double, and triple counts during the gating interval. Statistical analysis was applied to the counting data to deduce the true number of neutrons emitted per nuclear event, and from this the (γ, n) and $(\gamma, 2n)$ cross sections were calculated. More details of the experimental procedure are given in previous reports.^{9,10}

Pb^{206}

The Pb^{206} sample examined consisted of a 2-in.-diam metal disk weighing 100.38 g, and enriched to 99.77% Pb^{206} . Cross sections for (γ, n) and $(\gamma, 2n)$ reactions were measured and are given in Fig. 1. The peak $(\gamma, n) + (\gamma, np)$ cross section is 515 mb and occurs at 13.5 MeV, while the peak for the $(\gamma, 2n)$ cross section is 76 mb occurring at 17.5 MeV. The compound nucleus

⁸ C. P. Jupiter, N. E. Hansen, R. E. Shafer, and S. C. Fultz, Phys. Rev. **121**, 866 (1961).

⁹ S. C. Fultz, R. L. Bramblett, J. T. Caldwell, and N. A. Kerr, Phys. Rev. **127**, 1273 (1962).

¹⁰ S. C. Fultz, R. L. Bramblett, J. T. Caldwell, and C. P. Jupiter, Phys. Rev. **128**, 2345 (1962).

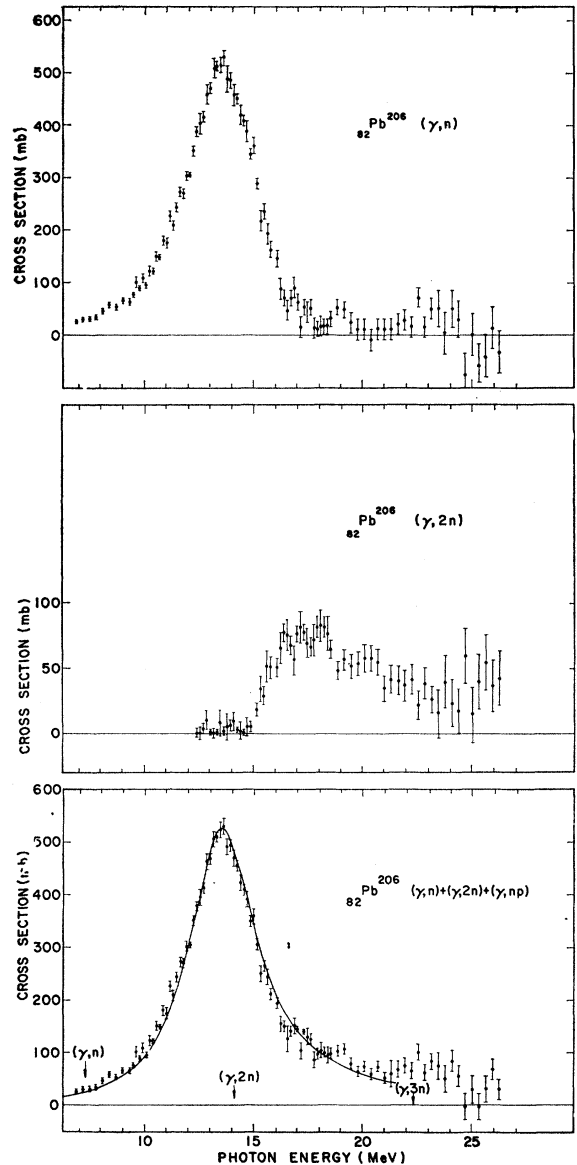


FIG. 1. Points shown in top figure are $\sigma[(\gamma, n) + (\gamma, np)]$ for Pb^{206} which was obtained from single-neutron counting data. Center figure shows data points for $\sigma(\gamma, 2n)$, obtained from double-neutron counting data. Bottom figure shows data for $\sigma[(\gamma, n) + (\gamma, np)] + \sigma(\gamma, 2n)$ for Pb^{206} , which represent the formation cross section for the compound nucleus. Solid curve is a plot of a Lorentz line having parameters given in Table II. The data are uncertain below 8 MeV owing to low beam intensities encountered

formation cross section $\sigma(\gamma, n) + \sigma(\gamma, 2n) + \sigma(\gamma, np)$ is also given in Fig. 1. Integrated cross sections for Pb^{206} are listed in Table I. That there was no evidence of structure in the giant resonance may be seen in Fig. 1. The width at half-maximum is 3.75 MeV. The solid line through the formation cross section data is a Lorentz line having the parameters given in Table II. The areas "W" under the wings of the Lorentz lines for energy regions below the threshold and above 28

TABLE I. Integrated cross sections in MeV-b, up to 28 MeV, for Pb isotopes and Bi.

Isotope	$\int_0^{28} \sigma(\gamma, n) dE$	$\int_0^{28} \sigma(\gamma, 2n) dE$	$\int_0^{28} \sigma dE$	$\int_0^{28} \sigma dE + W$	0.06NZ/A
Pb ²⁰⁶	2.22	0.56	2.78±0.28	3.07±0.36	2.96
Pb ²⁰⁷	2.05	0.60	2.65±0.27	2.95±0.30	2.97
Pb ²⁰⁸	1.96	0.95	2.91±0.29	3.21±0.32	2.98
Bi ²⁰⁹	2.17	0.76	2.93±0.29	3.25±0.33	3.00

MeV are included in the figures of the fifth column of Table I. Migdal's sum,¹¹ σ_{-2} , for Pb²⁰⁶ was found to be 15.6 ± 1.6 mb/MeV. The level density parameter¹² for the residual nucleus Pb²⁰⁵ was deduced from the ratio

TABLE II. Lorentz line parameters and σ_{-2} values for Pb isotopes and Bi.

Isotope	Peak σ_0 (mb)	Width Γ (MeV)	E_0 (MeV)	σ_{-2} (mb/MeV)	$0.00225A^{5/3}$ (mb/MeV)
Pb ²⁰⁶	525	3.75	13.7	15.6 ± 1.6	16.2
Pb ²⁰⁷	485	3.87	13.6	14.5 ± 1.5	16.3
Pb ²⁰⁸	495	3.78	13.6	14.1 ± 1.4	16.4
Bi ²⁰⁹	520	3.83	13.5	16.6 ± 1.7	16.6

of $\sigma(\gamma, 2n)$ to $\sigma[(\gamma, n) + (\gamma, np)] + \sigma(\gamma, 2n)$ and was found to be 6.6 ± 0.8 MeV⁻¹. The threshold for $\sigma(\gamma, 2n)$ was found to be 14.87 ± 0.15 MeV, which agrees with the value of 14.89 MeV given in Nuclear Data Sheets.¹³

Pb²⁰⁷

The Pb²⁰⁷ sample consisted of a 2-in.-diam metal disk weighing 98.95 g for which the isotopic enrichment of Pb²⁰⁷ was 92.8%. The measurements for $\sigma[(\gamma, n) + (\gamma, np)]$ and $\sigma(\gamma, 2n)$ are given in Fig. 2. From this it can be seen that the peak (γ, n) cross section is 475 mb occurring at 13.7 MeV while the peak $(\gamma, 2n)$ cross section is 80 mb at 17.0 MeV. Integrated cross sections are given in Table I. The nuclear formation cross section is also shown in Fig. 2, where it has been fitted with a Lorentz line with parameters given in Table II. The level density parameter for the residual nucleus Pb²⁰⁶ was found to be 13.5 ± 1.4 MeV⁻¹. The $(\gamma, 2n)$ threshold was found to be 14.44 ± 0.43 MeV, which is in fair agreement with the value 14.89 MeV,¹³ obtained by other methods.

Pb²⁰⁸

Measurements were made of $\sigma[(\gamma, n) + (\gamma, np)]$ and $\sigma(\gamma, 2n)$ for a 128.41-g sample of metallic Pb²⁰⁸ enriched

¹¹ J. S. Levinger, *Nuclear Photodisintegration* (Oxford University Press, London, 1960).

¹² J. Blatt and V. F. Weisskopf, *Theoretical Nuclear Physics* (John Wiley & Sons, Inc., New York, 1952).

¹³ *Nuclear Data Sheets*, compiled by K. Way *et al.* (Printing and Publishing Office, National Academy of Sciences—National Research Council, Washington, D. C., 1961).

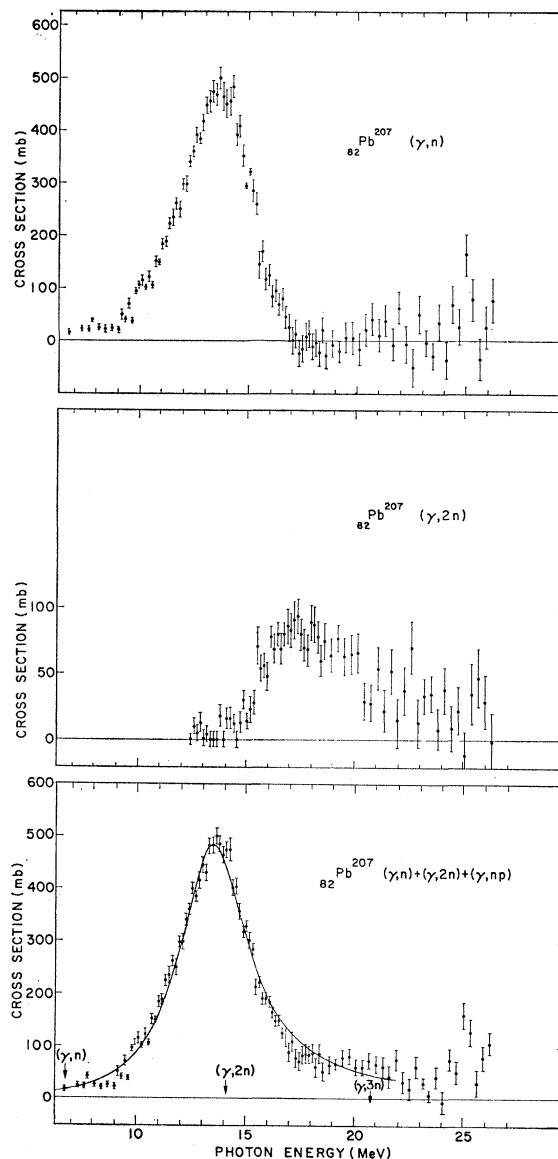


FIG. 2. Top figure shows data points for $\sigma[(\gamma, n) + (\gamma, np)]$ for Pb²⁰⁷, obtained from single-neutron counting data. Center figure shows data for $\sigma(\gamma, 2n)$ obtained from double-neutron counting data. Data points for the compound nucleus formation cross section of Pb²⁰⁷, i.e., $\sigma[(\gamma, n) + (\gamma, np)] + \sigma(\gamma, 2n)$ are shown in bottom figure. Solid curve is a plot of a Lorentz line having the parameters given in Table II. The data are uncertain below 8 MeV owing to low beam intensities encountered.

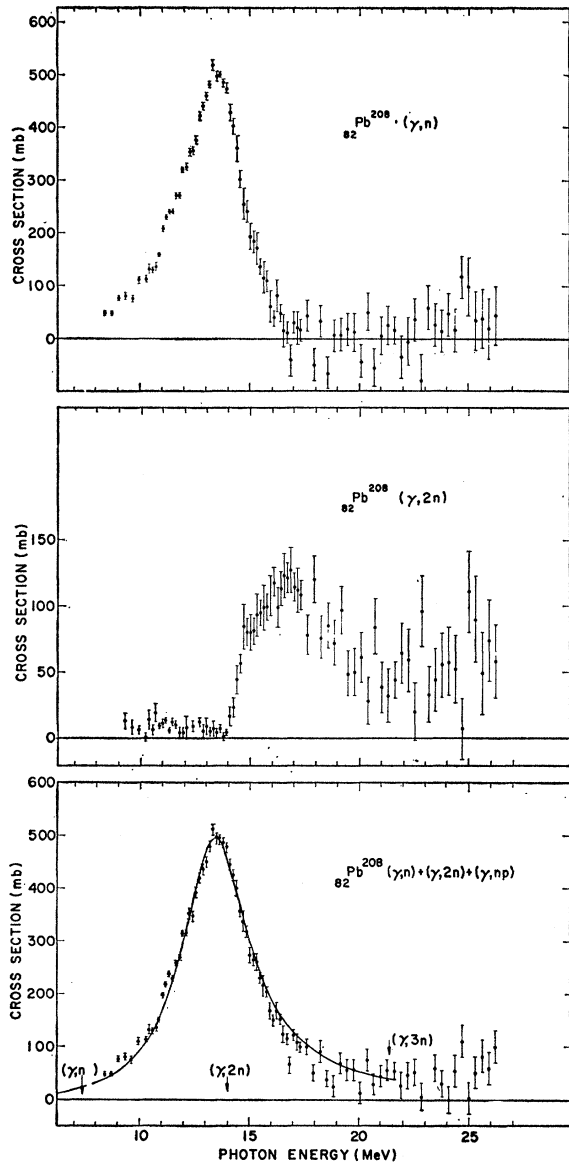


FIG. 3. Top figure shows data points for $\sigma[(\gamma,n) + (\gamma,np)]$ for Pb^{208} , obtained from single-neutron counting data. Center figure shows data for $\sigma(\gamma,2n)$ obtained from double-neutron counting data. Data points for the compound nucleus formation cross section of Pb^{208} , i.e., $\sigma[(\gamma,n) + (\gamma,np)] + \sigma(\gamma,2n)$ are shown in the bottom figure. Solid curve is a plot of a Lorentz line having the parameters given in Table II. The data are uncertain below 8 MeV owing to low beam intensities encountered.

to 99.75%. The cross sections obtained are given in Fig. 3. The peak for $\sigma[(\gamma,n) + (\gamma,np)]$ is 495 mb and occurs at 13.5 MeV while the peak value for $\sigma(\gamma,2n)$ is 117 mb at 16.5 MeV. Integrated cross sections for Pb^{208} are given in Table I. The compound nucleus formation cross section is also given in Fig. 3. This was fitted with a Lorentz line with parameters given in Table II.

Evidence for a small resonance at 11.5 MeV is apparent. The level density parameter for the residual

nucleus Pb^{207} was found to be $9.6 \pm 1.0 \text{ MeV}^{-1}$. The $(\gamma,2n)$ threshold was found to be $14.01 \pm 0.14 \text{ MeV}$, which compares favorably with the published value 14.11 MeV.¹³

Bi^{209}

The Bi^{209} sample consisted of a 2-in.-diam metal disk prepared from chemically pure bismuth. The results of measurements on $\sigma[(\gamma,n) + (\gamma,np)]$ and $\sigma(\gamma,2n)$ are given in Fig. 4. The peak value for $\sigma[(\gamma,n)$

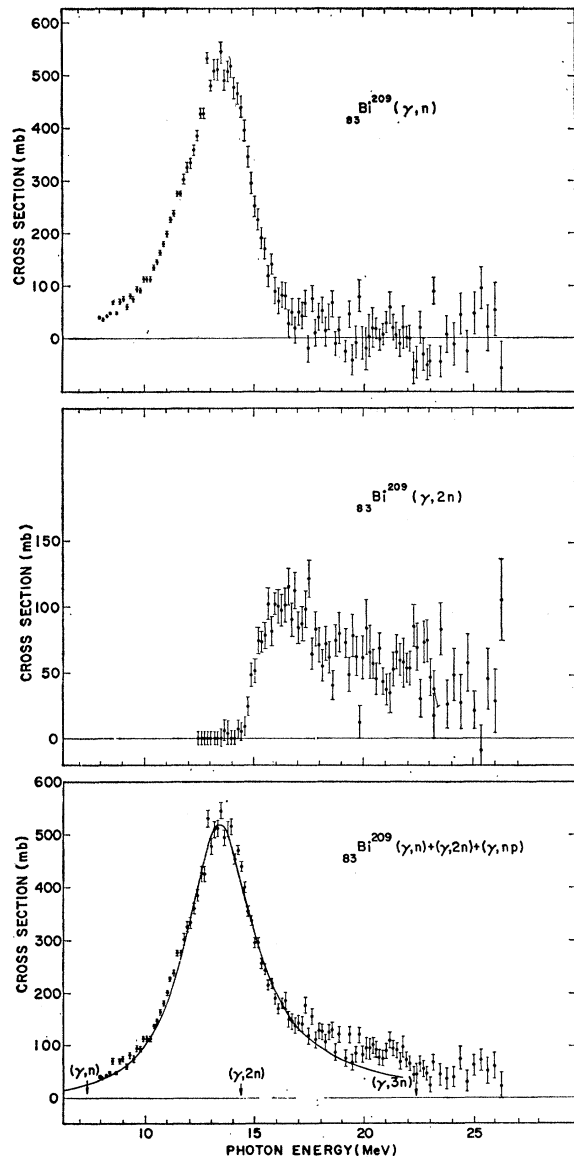


FIG. 4. Top figure shows data points for $\sigma[(\gamma,n) + (\gamma,np)]$ for Bi^{209} , obtained from single-neutron counting data. Center figure shows data for $\sigma(\gamma,2n)$ obtained from double-neutron counting data. Data points for the compound nucleus formation cross section of Bi^{209} , i.e., $\sigma[(\gamma,n) + (\gamma,np)] + \sigma(\gamma,2n)$ are shown in the bottom figure. Solid curve is a plot of a Lorentz line having the parameters given in Table II. The data are uncertain below 8 MeV owing to low beam intensities encountered.

$+(\gamma, np)]$ is 515 mb occurring at 13.5 MeV, while the peak value for $\sigma(\gamma, 2n)$ is 105 mb at 16.5 MeV. Integrated cross sections for Bi^{209} are given in Table I. The compound nucleus formation cross section is shown in Fig. 4. The data here have been fitted with a Lorentz line having the parameters given in Table II. No evidence of structure was present. The areas under the wings of the Lorentz lines, for energy regions below the threshold and above 28 MeV, are included in the figures of the fifth column of Table I. The level density parameter deduced for the residual nucleus Bi^{208} was found to be $10.2 \pm 0.9 \text{ MeV}^{-1}$. The $(\gamma, 2n)$ threshold was seen to be $14.5 \pm 0.14 \text{ MeV}$, which may be compared with 14.39 MeV obtained from data tables.¹³

DISCUSSION

Wilkinson¹⁴ has calculated the relative strengths of $E1$ transitions for Pb^{208} using the single-particle model. The neutron transitions having the greatest dipole strengths are $1h-1i$, $1i-1j$, $2f-2g$, and $3p-3d$, while the corresponding proton transitions are $1g-1h$, $1h-1i$, and $2d-2f$. These account for an integrated cross section of 2.26 MeV-b. Addition of the weaker transitions gives 2.47 MeV-b. This is somewhat below the integrated cross sections for the present experiment and those deduced from the sum rule, which are given in Table I. Wilkinson also deduced the fraction of (γ, p) reaction in the giant resonance to be 0.004 of the amount of (γ, n) reaction. A serious shortcoming of shell-model treatments is that the predicted energies of the levels constituting the giant resonances are very much lower than those measured experimentally. A shell-model treatment of Pb^{208} which utilizes the particle-hole concept has been achieved by Balashov *et al.*¹⁵ They have predicted the energies of the principal $E1$ transitions and have calculated their dipole strengths. The level with the greatest dipole strength occurs at 13.8 MeV, and accounts for 63% of the integrated cross section. This is in good agreement with the energy of the peak of the giant dipole resonance, i.e., 13.5 MeV. The total integrated cross section obtained by Balashov *et al.* is 3.79 MeV-b, which is somewhat greater than $3.21 \pm 0.32 \text{ MeV-b}$ obtained from the present experiment. Addition of the dipole component of the (γ, p) integrated cross section measured by Sorokin *et al.*⁷ would increase the integrated cross section by a factor of only 1.005, which is in agreement with Wilkinson's calculations.

Although the shell-model calculations on integrated cross sections are not in agreement with the present measurements, it is evident from Table I that the measured values agree well with those deduced from the Thomas-Reiche-Kuhn sum rule. It is evident, too,

from Figs. 1 to 4 that the giant resonances obtained in the manner outlined in this report can be fitted with Lorentz lines. The wing corrections to the integrated cross sections, denoted as " W " in the fifth column of Table I (which are deduced from the Lorentz curves) add approximately 10% to the integrated cross sections, but do not alter the agreement with the sum rule.

The widths of the giant resonances show little change with increasing nucleon number. The values for σ_{-2} are shown in the fifth column of Table II. In most cases they agree with the σ_{-2} values theoretically derived, which are given in the sixth column. Variation in the level density parameters " a " with single nucleon changes may be seen in Table III. The residual nucleus

TABLE III. Level density parameters a .

Residual nucleus	Reaction	Excitation energy (MeV)	a (MeV ⁻¹)	Reference
Pb^{205}	(γ, n)	5.9	6.6 ± 0.7	a
Pb^{206}	(n, n')	5.2	6.1	b
	(γ, n)	8.2	13.5 ± 1.5	a
Pb^{207}	(n, γ)	6.7	10.52	c
	(γ, n)	6.5	9.6 ± 1.0	a
Bi^{208}	(γ, n)	6.1	10.2 ± 1.1	a
Bi^{209}	(n, n')	5.0	4.5	b

^a Present work.
^b See Ref. 16.
^c See Ref. 17.

Pb^{205} has a lower " a " value than the other isotopes examined in the present work. This deviation is significant in view of the 11% statistical uncertainty.

It is difficult to compare these values for the level density parameter with those obtained by other methods, since the latter vary greatly. Thompson¹⁶ and Erba *et al.*¹⁷ have tabulated values of " a " for various excitation energies and nuclei. Those listed in Table III for comparison with the present (γ, n) results were deduced by use of the Weisskopf¹² method, without pairing correction.

The results of the present experiment indicate that in the case of isotopes of high atomic numbers there is only minor influence of single nucleons upon the photo-neutron cross sections of isotopes one or two nucleons removed from neutron or proton closed shells. The integrated cross sections agree well with those deduced from saturation of the dipole sum rule, with no corrections for the exchange force. In addition the values for σ_{-2} are in agreement with those deduced from a relatively simplified theoretical treatment. Values for the level density parameters show a wide dispersion. The narrow widths of the giant resonances indicate that

¹⁴ D. H. Wilkinson, *Physica* **22**, 1039 (1956).

¹⁵ V. V. Balashov, V. G. Shevchenko, and N. P. Yudin, *Zh. Eksperim. i Teor. Fiz.* **41**, 1929 (1961) [English transl.: *Soviet Phys.—JETP* **14**, 1371 (1962)].

¹⁶ D. B. Thompson, *Phys. Rev.* **129**, 1649 (1963).

¹⁷ E. Erba, U. Facchini, and E. Saetta Menichella, *Nuovo Cimento* **22**, 1237 (1961).

the nuclei examined are not deformed, but are essentially spherical in shape.

ACKNOWLEDGMENTS

The authors wish to express their thanks to the operating crew, electronic maintenance crew, and to the

mechanical technicians, for their cooperation during the experiment. They are also grateful to Dr. G. Rogosa and the AEC Cross Section Isotopes Pool for loan of the enriched isotopes. Finally, they wish to acknowledge theoretical help given by Dr. F. Buskirk of the Naval Post Graduate School at Monterey.

Polarization of Neutrons from the $N^{14}(d,n_0)O^{15}$ Reaction*

H. M. EPSTEIN,[†] D. F. HERRING,[‡] AND K. W. JONES[§]

The Ohio State University, Columbus, Ohio

(Received 18 May 1964)

The polarization of neutrons from the $N^{14}(d,n_0)O^{15}$ reaction has been measured at 1.32 MeV for laboratory angles from 0 to 90 deg. The polarization is positive (using the Basel sign convention) and has a maximum value of about 0.10 at 30 deg. The neutrons were produced by bombardment of a 220-keV-thick nitrogen gas target with deuterons from The Ohio State University electrostatic accelerator. The polarization of the neutrons was determined by a measurement of the left-right asymmetry in the scattering of the neutrons from a liquid-helium scintillation counter. Time-of-flight and pulse-shape discrimination techniques were used to reduce the background. Compound nucleus and distorted-wave Born-approximation direct interaction calculations were carried out and compared with the polarization data as well as with the available differential cross-section measurements.

1. INTRODUCTION

A MEASUREMENT of the polarization of the neutrons from the $N^{14}(d,n_0)O^{15}$ reaction at low energies is of interest for several reasons. The interaction mechanism for the $N^{14}(d,n_0)O^{15}$ reaction and the mirror reaction $N^{14}(d,p_0)N^{15}$ is uncertain at bombarding energies below 2 MeV. The excitation curves, particularly for the $N^{14}(d,n_0)O^{15}$ reaction, show peaks which can be correlated with states in the O^{16} compound nucleus measured by other means. The angular distributions have been interpreted as evidence for a few-level compound nucleus reaction¹ and for plane-wave exchange stripping.^{2,3} The addition of polarization data might help to distinguish between the compound nucleus and stripping interaction mechanisms.

If the reaction should proceed in large part by compound nucleus formation, it might also be possible to extract the parameters of the compound states involved. For deuteron bombarding energies around 2-MeV states in O^{16} around 22.7 MeV would be excited. This excitation energy is near that of the giant dipole resonance observed in the photodisintegration of O^{16} . The properties of the giant dipole state have recently

been of considerable theoretical interest,⁴ and additional experimental knowledge of the parameters of the excited states in this energy region should be useful.

The $N^{14}(d,n_0)O^{15}$ reaction has been used as a source of neutrons of energies around 6 MeV. It is not as convenient a source of neutrons as the $D(d,n)He^3$ or the $T(p,n)He^3$ reactions because of its substantially lower cross section and the lower energy neutrons produced in the $N^{14}(d,n)O^{15}$ reactions and the gamma rays resulting from the (d,n) , (d,p) , and (d,α) reactions. However, if the neutrons from the $N^{14}(d,n_0)O^{15}$ reaction are highly polarized, the reaction might still be of interest as a source of polarized neutrons.

2. EXPERIMENTAL METHOD

The neutrons from the $N^{14}(d,n_0)O^{15}$ reaction were produced by bombardment of a N^{14} gas target with deuterons from The Ohio State University electrostatic accelerator. The gas target was a 0.010-in. stainless steel tube with a tantalum beam stop and a 1.27- μ nickel entrance foil. The target length was 1.2 cm and the target pressure 0.5 atm. The energy loss of the beam in traversing the target gas filling was about 220 keV. The resulting average beam energy was 1.32 MeV. Beam currents of about 0.7 μ A were used. It was originally planned to make measurements on the peak in the zero-degree excitation curve at 1.5 MeV, but this was impossible because of limitations in accelerator performance. The 1.32-MeV energy actually

* Work supported in part by the U. S. Atomic Energy Commission and The Ohio State University Development Fund.

[†] Supported by Battelle Memorial Institute fellowship. Present address: Battelle Memorial Institute, Columbus, Ohio.

[‡] Present address: General Atomic, San Diego, California.

[§] Present address: Brookhaven National Laboratory, Upton, New York.

¹ W. M. Jones, Nucl. Phys. 26, 203 (1961).

² J. L. Weil and K. W. Jones, Phys. Rev. 112, 1975 (1958).

³ T. Retz-Schmidt and J. L. Weil, Phys. Rev. 119, 1079 (1960).

⁴ See, for example, G. E. Brown, L. Castillejo, and J. A. Evans, Nucl. Phys. 22, 1 (1961).